[Journal of the Faculty of Science, Hokkaidô University, Japan, Ser. VII. Vol. II, No. 4, 1966]

Note on Aeromagnetic Survey with Special Reference to Volcanic Regions (Part 1)

Izumi YOKOYAMA

(Received July 31, 1966)

Abstract

Merits of aeromagnetic surveys are speediness in their practice and possibility of eliminating topographical effects. The latter depends on flight heights over topographies and their magnetization. Topographical effects are usually disadvantageous for the aim of surveys but, in some cases, those due to volcanic structures are the purpose of surveys.

In this paper, the discussion on aeromagnetic surveys are confined to ones of total force. Profiles of magnetic anomaly in total force at various heights over a dipole are examined. Some examples of aeromagnetic surveys affected by the topographies are mentioned. A method of analysis of total force anomaly is presented: anomaly is attributed to magnetic mass concentrated on a subterranean plane and with some approximations, probable mass distributions are obtained directly from total force anomalies. An example of the analysis is shown for the result of the survey on Lake Towada though the survey is shipborne.

1. Total force anomaly to be observed over a magnetic dipole

Magnetic anomalies over volcanic structures consist of those due to the cones above the surroundings and those due to the deeper parts beneath the bottoms of the cones. The former is deemed, in a sense, as topographic effects. As the most fundamental model for all-inclusive subterranean sources, a magnetic dipole is dealt with in the following:

Magnetic potential due to a dipole is expressed as

$$V = -\frac{M\cos\theta}{r^2}$$

where M is moment of dipole, r distance from the dipole, and θ angle between r and the direction of magnetization. Then total force anomaly ΔF is obtained as

$$\Delta F = \frac{M}{r^3}\sqrt{3\cos^2\theta+1}\ .$$

If a dipole is replaced by a uniformly magnetized sphere, M is expressed as

$$M = \frac{4}{3}\pi R^3 \Delta\kappa \cdot F,$$

where $\Delta\kappa$ is susceptibility contrast, R radius of the sphere, and F total force of geomagnetic field. Then we get

$$\Delta F = \frac{4}{3}\pi \Delta\kappa F \left(\frac{R}{r}\right)^3 \sqrt{3\cos^2\theta + 1}\ .$$

If flight height is measured by R, radius of the sphere, the distributions of relative total force anomaly in the north-south direction at various heights over a dipole are estimated as shown in Fig. 1 where the dipole is magnetized in

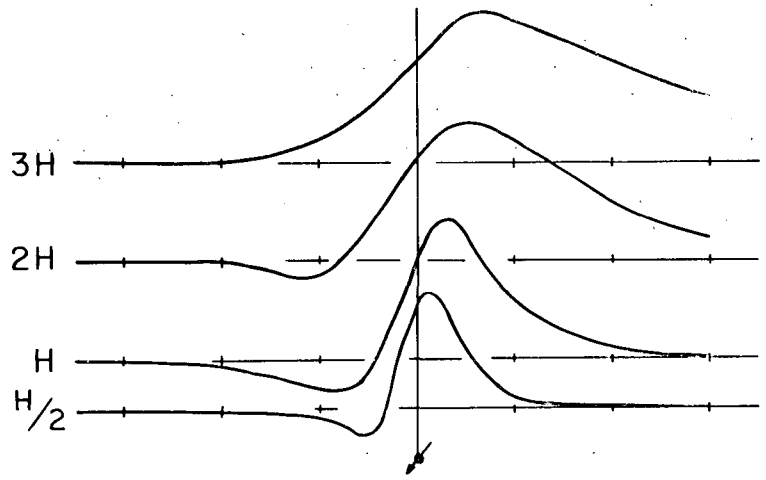

Fig. 1. Distribution of total force anomaly over a dipole which is magnetized in the direction of inclination (57°). Anomalies right over the dipole are normalized to be be unity.

the direction of inclination (57°) and the anomalies right over the dipole are normalized to be unity in order to examine their modes. If we assume $\Delta\kappa = 10^{-3}$c.g.s. and $F = 0.5\Gamma$, the maximum anomalies at respective heights in Fig. 1 are 2956, 370, 46 and 14γ respectively.

As a practical problem, it may be useful to know a relation between apparent wave-length of anomaly and depth of an assumed dipole. From the profiles shown in Fig. 1, a rough relation is obtained and shown in Fig.

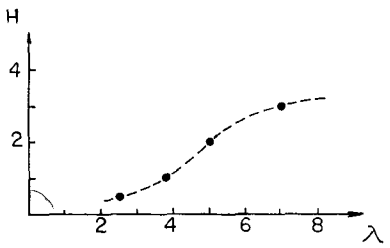

Fig. 2. Relation between apparent wave-length of anomaly λ and depth of a dipole H deduced from Fig. 1.

2 where both the wave-length λ and the depth H are measured by R. As the flight height becomes higher, the wave-length increases more rapidly and of course, the amplitude decreases. In other words, geomagnetic anomalies of short wave-length represent the effects of topographies or of geologic structures of shallow depth while the ones of long wave-length do the effects of deeper

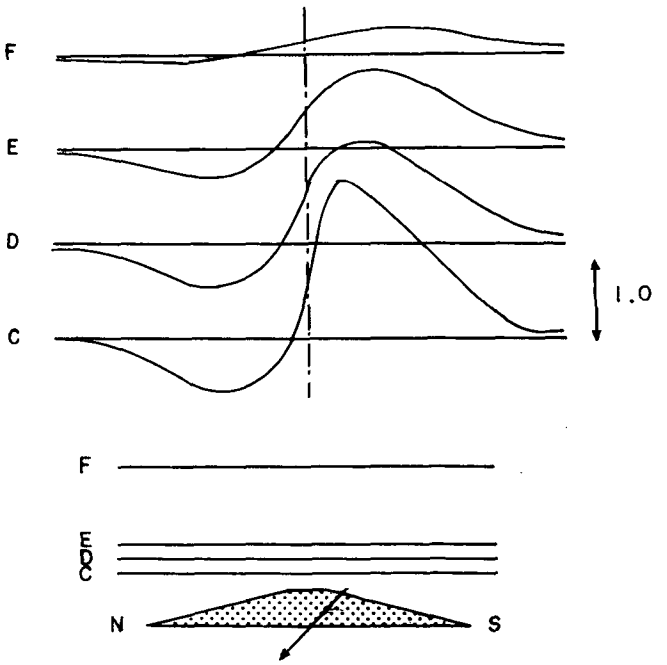

Fig. 3. Profiles of total force anomaly along the north-south line passing through the center of a magnetized cone of which the slope is 15° (after T. Rikitake and Y. Hagiwara).

and larger structures.

On the other hand, T. Rikitake and Y. Hagiwara[1] calculated total force anomaly over a magnetized circular cone. Some of their results are shown in Fig. 3 where the direction of magnetization agrees with that of inclination (48°) and the intensity of magnetization and the bottom radius are taken as unity. The flight heights are taken as 0.3, 0.4, 0.5 and 1.0. In the figure, apparent wave-lengths of the anomalies are not so conspicuously different from the diameter of the cone although phases of magnetic anomalies are different each other according to their heights.

2. Examples of topographical effects on aeromagnetic surveys

Generally speaking, volcanic structures are not limited to the volcanic cones above the surrounding terrains and include the subterranean parts beneath the cones. Their contributions to the aeromagnetic anomalies depend on their structures and magnetization of the rocks composing the structures. It is useful to distinguish between the effects of volcanic cones and of subterranean parts. In this section, this problem is discussed by examples.

Magnetic survey on and over Lake Sikotu

Lake Sikotu is a caldera lake in Hokkaido, surrounded by volcanic cones. The subterranean structure of this caldera was already investigated by the

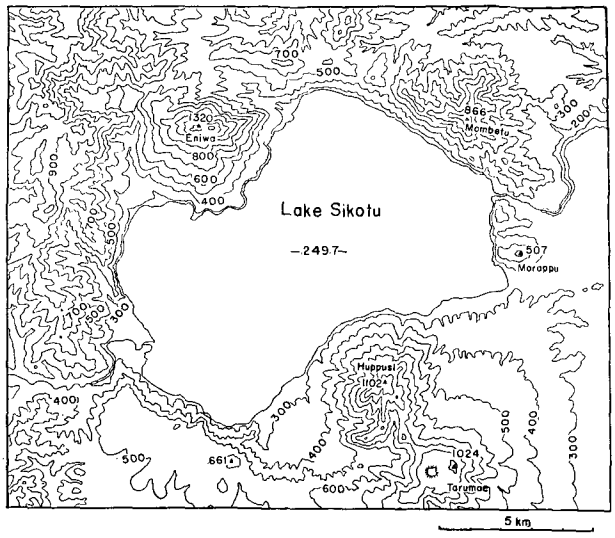

Fig. 4. Topography around the Sikotu caldera lake. (contours in meter)

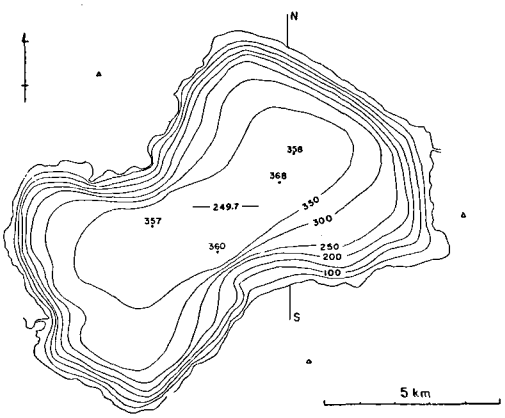

Fig. 5. Depth contours of Lake Sikotu in meters.

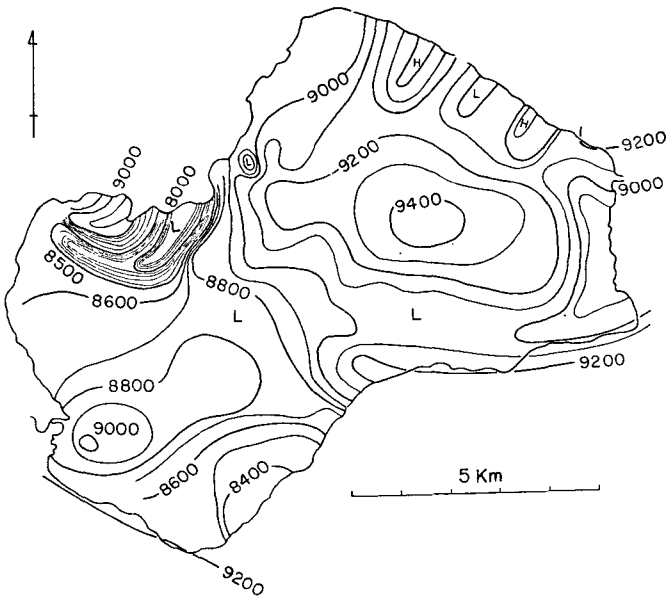

Fig. 6. Distribution of the total magnetic force on Lake Sikotu. Each numeral should be added to 40,000 gamma.

present author[2]. As for the geomagnetic studies, shipborne surveys by a proton magnetometer were carried out on the lake in 1962 and 63, while an airborne survey by a flux-gate magnetometer was made over the lake in 1964 by the Geological Survey of U.S.A. Comparison of the results of the above

surveys is interesting to us for knowing the effectiveness and limit of aeromagnetic surveys.

Topographies around Lake Sikotu and depth-contours of the lake are shown in Figs. 4 and 5 respectively. The distribution of geomagnetic total force on the lake obtained by the shipborne surveys is shown in Fig. 6. The Geological Survey of U.S.A. carried out an aeromagnetic survey in eight directions intersecting each other at the centre of the lake at an elevation of 500 meter above terrain and they got eight profiles represented by relative values. Using these profiles, the present author draws a tentative horizontal contours relative to the intersection point as shown in Fig. 7. In the figure, the anomalies due to the steep volcanic cones are conspicuous at first sight and are predominant even over the lake, especially in the western part. Volcano Eniwa shows a typical pattern of geomagnetic anomaly due to a

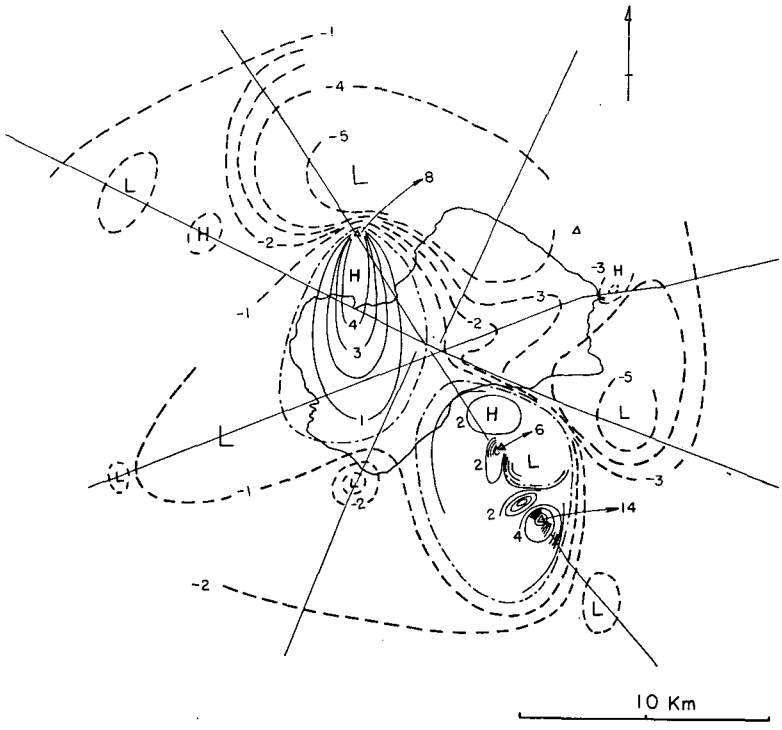

Fig. 7. A tentative distribution of total force anomaly relative to th centre of the lake at a height of 500 meter above terrain deduced from eight profiles surveyed by the U.S.G.S. Unit is 100γ.

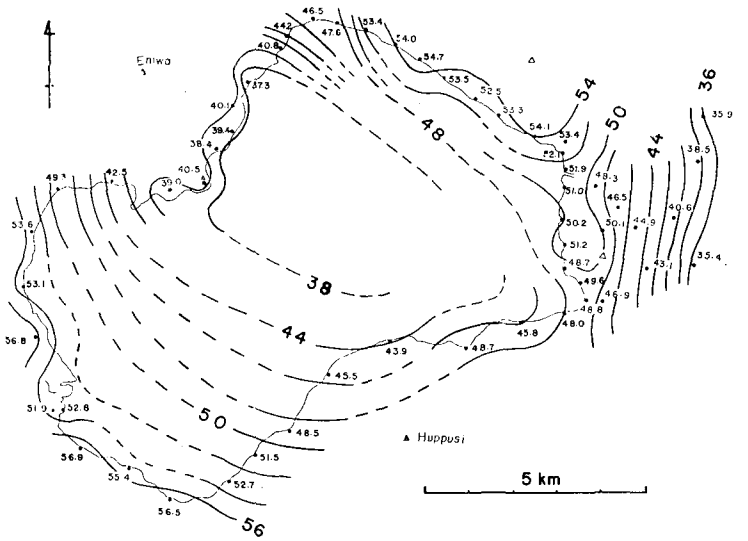

Fig. 8. *Bouguer gravity anomaly in milligal (not corrected for topography).*

normally magnetized cone and Volcano Tarumae of which lava dome was formed by the eruption in 1910, causes irregular anomalies. Comparing Fig. 6 with Fig. 7, one notices that these are significantly different from each other except that the contours of -200 and -300γ in the air which protrude eastward from the centre of the lake as a relative high, may correspond to the high of 49400γ observed on the water.

For reference, the distribution of the Bouguer gravity anomaly deduced from the land measurements along the coast line of the lake is shown in Fig. 8 where figuring the general aspect of the gravity field around and also on the lake is fortunately successful. On Lake Sikotu, positive magnetic anomalies accompanied by low gravity anomalies are observed as shown in Figs. 6 and 8. Magnetic anomaly and gravity anomaly are generally related by Poisson's theorem, which states that magnetic potential is proportional to gravity component in the direction of magnetization. It is ambiguous whether both the anomalies on Lake Sikotu are caused by the same origin or not. However, the two kinds of anomalies contradict each other in their patterns; the gravity anomaly has a unicentred pattern while the magnetic anomaly two maximums. These anomalies can not be interpreted combinedly by Poisson's theorem which assumes uniform magnetization of causative material. Therefore, it may be concluded that the origins of the two anomalies are different. Thus,

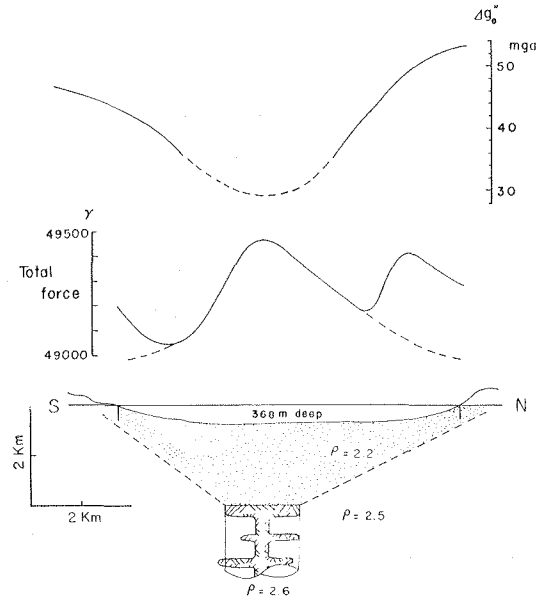

Fig. 9. Profiles of observed anomalies and deduced subterranean structure along line NS shown in Fig. 5.

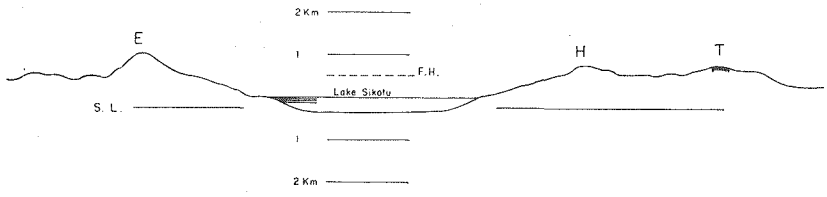

Fig. 10. Topographical profile along a line passing Eniwa, the centre of the lake, Huppusi and Tarumae. F.H. denotes the flight height.

in the writer's previous paper, the subterranean structure is surmised as shown in Fig. 9.

Fig. 10 shows the topographical profile along a line passing Eniwa, the centre of the lake, Huppusi and Tarumae. At the centre of the lake, 500 meter above the lake water, geomagnetic field is almost equally influenced by the surrounding volcanoes and by the subterranean magnetic source of which top is at a depth of about 2 km below the lake surface as shown in Fig. 9. A similar example is found above the caldera of Kuril Lake in Kamchatka

surveyed by G.S. Steinberg and L.A. Rivosh[3].

If the geomagnetic studies of Eniwa, Huppusi and Tarumae are aimed, an aeromagnetic survey may be useful. However, for the study of the geomagnetic anomaly caused by the caldera structure of Sikotu, a shipborne survey on the lake is more effective because the post-caldera volcanoes seriously disturb the geomagnetic field over the lake.

Magnetic and topographic profiles in the eastern part of Hokkaido

In 1964, the Geological Survey of U.S.A. made a reconnaisance survey of magnetic total force over the eastern part of Hokkaido where there are many

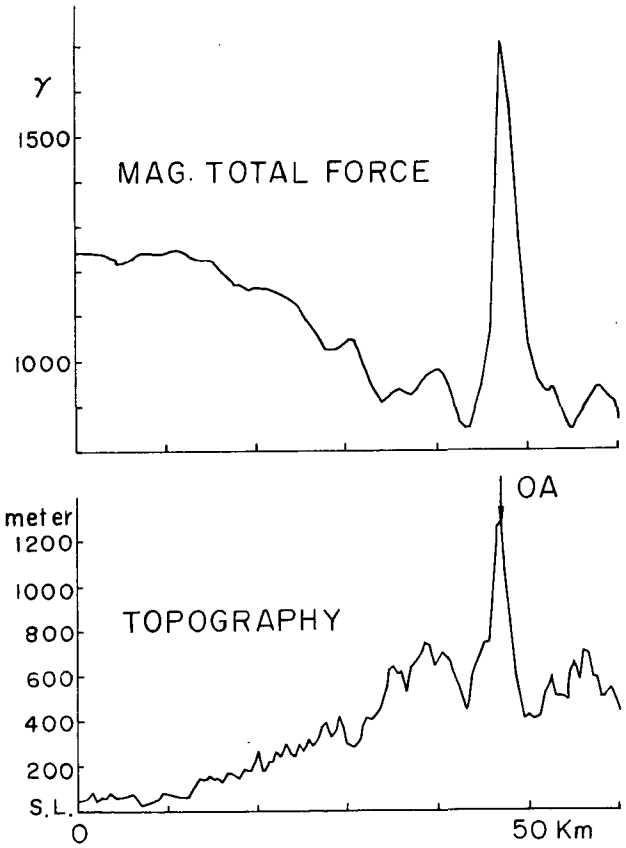

Fig. 11. Profiles of magnetic total force and topography along a line passing Volcano O-Akan (OA) in the north-south direction.

volcanic structures. In the following, the author mentions two magnetic profiles constructed from the contours offered by the Geological Survey, for examples to discuss topographical effects on geomagnetic anomalies in total force. At both the profiles, the flight height was 1800 meter above sea level.

Fig. 11 shows the profiles of magnetic total force and topography along a northward line passing Volcano O-Akan. In the figure, the topographic profile represents the running average over 41 readings of altitude at the horizontal distance of every 500 meter. In order to find a predominant wavelength at a certain point of the above profiles, they are modified as follows:

The original profile is expressed by $f(x)$, a part of which is to be analyzed around $x=x_o$. $f(x)$ is multiplied by a weight function $K(x)$, which is chosen as

$$K(x)=e^{-c^2(x-x_0)^2/4}.$$

A modified profile $F(x)=f(x)\cdot K(x)$ is practically equal to $f(x)$ in the neighbourhood of $x=x_o$, but tends to zero when $(x-x_o)$ becomes $\pm\infty$. In the present case, $K(x)$ is chosen in such a way that it diminishes to 1/2 at a distance of

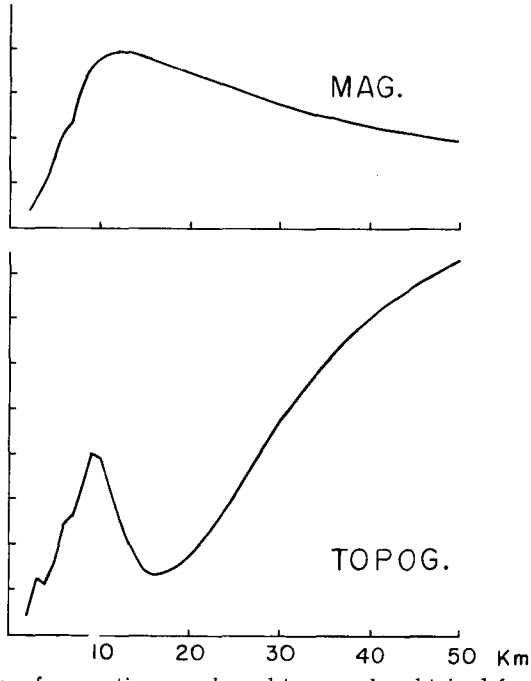

Fig. 12. Spectra of magnetic anomaly and topography obtained for O-Akan. Units of the ordinates are arbitrary.

12.5 km from x_0. Thus an isolated wave-form conserves well the spectral structure of the part of $f(x)$ concerned. The spectrum of such an isolated wave-form is obtainable by means of Fourier analysis. The spectra of magnetic anomaly and topography obtained for Volcano O-Akan are shown in Fig. 12 where a magnetic anomaly of 12 km in wave-length is clearly correlated with a topography of 9 km in wave-length.

Fig. 13 shows the profiles of magnetic total force and topography along a line passing Volcanoes Nisibetu and Etobi in the north-south direction. The same analysis to the previous example is made for Nisibetu and the spectra are obtained as shown in Fig. 14: the magnetic anomaly has a predominant wave-length of about 15 km while the topography has not so

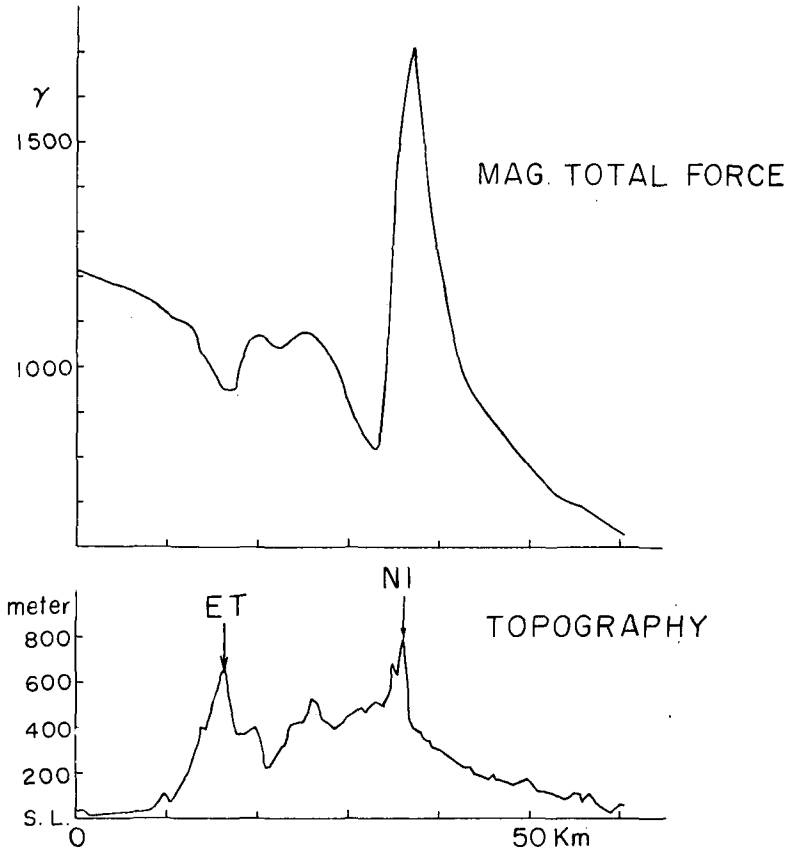

Fig. 13. Profiles of magnetic total force and topography along a line passing Volcanoes Etobi (ET) and Nisibetu (NI) in the north-south direction.

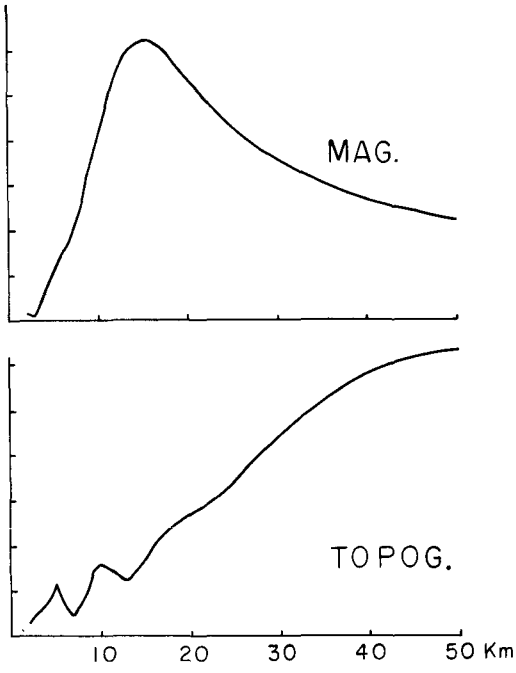

Fig. 14. Spectra of magnetic anomaly and topography obtained for Nisibetu.

predominant wave-length except small ones of 5 and 10 km. In consideration of the flight level, being higher than the top of Nisibetu by about 1000 meter, a remarkably high anomaly amounting to 1000γ is not due to Nisibetu itself but due to local effects of which origin is rather deep beneath the undulation of topographies.

The spectra obtained for Etobi are shown in Fig. 15: the magnetic anomaly has predominant wave-lengths of 15 and 8 km, the former being the adjacent wave-form and the latter negative. The topography has a predominant wave-length of 10 km. Thus the positive topography causes the negative magnetic anomaly amounting to about 120γ: This may be interpreted by the assumption that magnetization of rocks of Etobi is reverse to the present geomagnetic field.

3. A method of analysis of total force anomaly

In surveys of geomagnetic total force, we measure magnitude of total force vector except the direction of the vector. In other words, such measure-

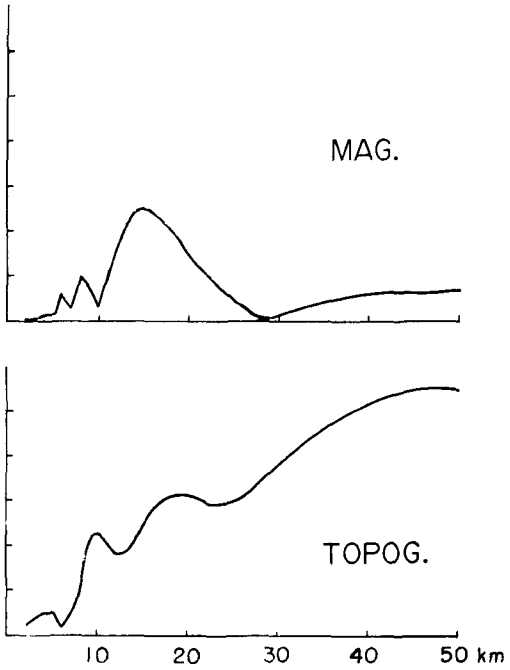

Fig. 15. Spectra of magnetic anomaly and topography obtained for Etobi.

ments are not complete as a geomagnetic measurement and therefore we must provide some approximations in their quantitative analyses.

A practical method of aeromagnetic interpretation was already proposed by V. Vacquier and others[4] who assumed various models of soruces and calculated numerically total force anomalies. And I. Zietz and R.G. Henderson[5] made model experiments to devise a rapid method for calculating magnetic anomalies of three-dimensional structures. Recently T. Rikitake and Y. Hagiwara[1] calculated magnetic anomalies over magnetized circular cones as already mentioned.

In contrast to the above model methods, C. Tsuboi and T. Fuchida[6] proposed a method of finding the density distribution concentrated on a subterranenan plane directly from the gravity anomalies observed on the earth's surface. T. Nagata[7] extended this method to the anomalies in each component of magnetic force. Theoretically, it is not possible to determine unique solution of mass distribution from the magnetic field observed on a plane alone. It is not impossible, however, to find a satisfactory solution for

the observation, if some assumptions being not improbable geophysically and geologically, are made.

In this section, the above method of potential is extended to magnetic anomalies in total force and the discussion is confined to a two-dimensional case for the sake of simplicity. Surface density of magnetic material concentrated on a subterranean plane at a depth of d is expanded into Fourier series as

$$\Delta\rho(x) = \sum_m (C_m \cos m x + S_m \sin m x) . \tag{1}$$

Gravitational potential due to the above mass is expressed as

$$\Delta W(x) = 2\pi G \sum \frac{e^{mz}}{m} (C_m \cos m x + S_m \sin m x) , \tag{2}$$

where G is the gravitational constant and z is positive downwards. At the surface ($z=-d$), the horizontal and vertical components are given as follows:

$$\Delta X = \frac{1}{G(\sigma-\sigma_0)} \left\{ \alpha \frac{\partial^2 W}{\partial x^2} + \gamma \frac{\partial^2 W}{\partial x \partial z} \right\} , \tag{3}$$

$$\Delta Z = \frac{1}{G(\sigma-\sigma_0)} \left\{ \alpha \frac{\partial^2 W}{\partial x \partial z} + \gamma \frac{\partial^2 W}{\partial z^2} \right\} , \tag{4}$$

where $(\sigma-\sigma_0)$ is density contrast and α and γ denote the horizontal and vertical intensities of magnetization of the magnetic material on the plane.

Observed total force anomaly ΔT is expressed as

$$\Delta T = \sqrt{(X_0+\Delta X)^2 + (Z_0+\Delta Z)^2} - \sqrt{X_0^2+Z_0^2} . \tag{5}$$

When a difference vector $\overline{\Delta T}$ connecting the points of the original and resultant vectors is introduced (Fig. 16), the magnitude of the vector $\overline{\Delta T}$ is expressed as

$$\overline{\Delta T} = \sqrt{(\Delta X)^2 + (\Delta Z)^2} . \tag{6}$$

If dip angle remains unchanged, $\overline{\Delta T}$ is exactly equal to ΔT, and when the changes in dip angle are the same, $\overline{\Delta T}$ may be the better approximated to ΔT for the larger ΔT and the worse for the smaller ΔT.

On the other hand, when only dip angle changes without any changes in magnitude of total force, we measure $\Delta T=0$; These changes can not be

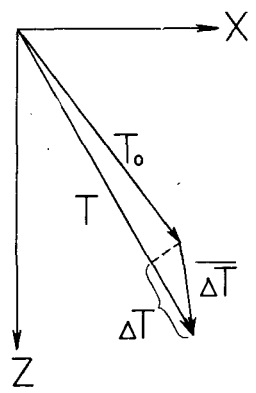

Fig. 16. A difference vector $\overline{\Delta T}$ and a change of total force ΔT.

detected by total force surveys. Therefore, we assume that the measurement $\Delta T=0$ means simply $\overline{\Delta T}=0$ (no changes in vector). Thus we may write as follows:

$$\Delta T \fallingdotseq \overline{\Delta T} \ . \tag{7}$$

Introducing (3) and (4) into (7) and (6), one gets

$$\Delta T = \frac{J}{G(\sigma-\sigma_0)} \sqrt{\left(\frac{\partial^2 W}{\partial x \partial z}\right)^2+\left(\frac{\partial^2 W}{\partial x^2}\right)^2} = \sqrt{\frac{\Delta T_1{}^2+\Delta T_2{}^2}{2}} \ , \tag{8}$$

where J denotes intensity of magnetization ($J=\sqrt{\alpha^2+\gamma^2}$) and ΔT_1 and ΔT_2 are represented as follows:

$$\Delta T_1 = \frac{J}{G(\sigma-\sigma_0)} \left\{\frac{\partial^2 W}{\partial x^2} + \frac{\partial^2 W}{\partial x \partial z}\right\}, \tag{9}$$

and

$$\Delta T_2 = \frac{J}{G(\sigma-\sigma_0)} \left\{\frac{\partial^2 W}{\partial z^2} + \frac{\partial^2 W}{\partial x \partial z}\right\}. \tag{10}$$

By eq. (2), ΔT_1 and ΔT_2 are converted into the following trigonometric series:

$$\Delta T_1 = \frac{2\pi J}{(\sigma-\sigma_0)} \sum m e^{-md} \left[(S_m-C_m)\cos m x-(C_m+S_m)\sin m x\right], \tag{9'}$$

and

$$\Delta T_2 = \frac{2\pi J}{(\sigma-\sigma_0)} \sum m e^{-md} \left[(S_m+C_m)\cos m x+(S_m-C_m)\sin m x\right]. \tag{10'}$$

On the other hand, the observed result of total force is expanded into a

Fourier series as follows:

$$\Delta T = \sum_m (A_m \cos mx + B_m \sin mx) . \tag{11}$$

Equating this equation with (8), one may determine coefficients C_m and S_m expressed in the terms of A_m and B_m when the right hand side of (8) can be converted into linear combinations of ΔT_1 and ΔT_2. If we may assume some appropriate relations between ΔT_1 and ΔT_2, the above condition may be satisfied. Several examples are mentioned as follows:

1) $\Delta T_2 = 0 : \Delta T = \dfrac{\Delta T_1}{\sqrt{2}}$,
$$\begin{cases} C_m = -\dfrac{\sqrt{2}(\sigma-\sigma_0)}{4\pi J} \dfrac{e^{md}}{m} (A_m + B_m) , \\ S_m = \dfrac{\sqrt{2}(\sigma-\sigma_0)}{4\pi J} \dfrac{e^{md}}{m} (A_m - B_m) . \end{cases}$$

2) $\Delta T_1 = 0 : \Delta T = \dfrac{\Delta T_2}{\sqrt{2}}$,
$$\begin{cases} C_m = \dfrac{\sqrt{2}(\sigma-\sigma_0)}{4\pi J} \dfrac{e^{md}}{m} (A_m - B_m) , \\ S_m = \dfrac{\sqrt{2}(\sigma-\sigma_0)}{4\pi J} \dfrac{e^{md}}{m} (A_m + B_m) . \end{cases}$$

3) $\Delta T_1 = \Delta T_2 : \Delta T = \dfrac{1}{2} (\Delta T_1 + \Delta T_2)$,
$$\begin{cases} C_m = -\dfrac{(\sigma-\sigma_0)}{2\pi J} \dfrac{e^{md}}{m} B_m , \\ S_m = \dfrac{(\sigma-\sigma_0)}{2\pi J} \dfrac{e^{md}}{m} A_m . \end{cases}$$

4) $\Delta T_1 = n \Delta T_2 : \Delta T = \sqrt{\dfrac{n^2+1}{2}} \cdot \dfrac{1}{n+1} (\Delta T_1 + \Delta T_2)$, ...

In order to get a probable distribution of magnetic material, we are obliged to make an appropriate assumption of the relation between ΔT_1 and ΔT_2 because we observe the only total force for the three geomagnetic components, in other words, only magnitude of a vector quantity.

Total force measurements on Lake Towada

Lake Towada is a caldera lake in Tōhoku district. Inside the caldera, there is a inner crater bounded by two peninsulas. The measurements were carried out by a proton precession magnetometer tugged by a boat in August, 1963. Fig. 17 shows depth contours and the measuring courses, one of which (AB) passes the inner crater (Nakano-Umi) and the middle of the cladera lake. The total force profiles along AB an AC-lines are shown in Fig. 18 with the bottom profiles. Course AC passes by a peninsula which forms a part of the crater wall and therefore, the anomalies near the coast and at shallow

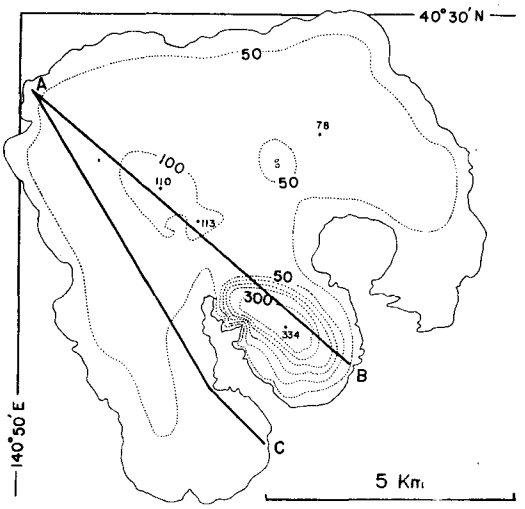

Fig. 17. Depth contours in meter and the measuring courses at Lake Towada.

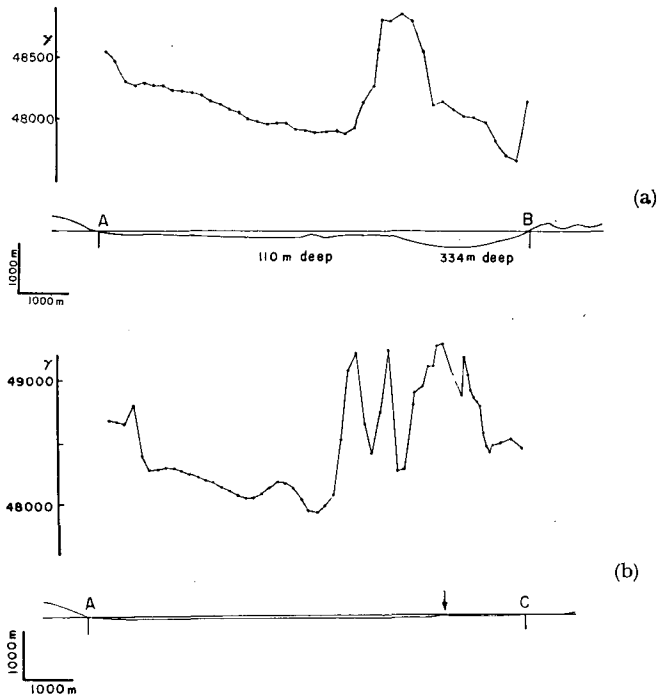

Fig. 18. Profiles of total force and bottom profiles of Lake Towada.

depths are rather irregular and large. In the following, the anomaly along AB-line is analyzed by the before-mentioned method. The average intensity of magnetization of the rock specimens collected from the surrounding coast and the islets (Gomonseki) in the middle of the lake is 1.3×10^{-3} emu/cc.

Total force anomaly along AB-line is obtained by subtraction of regional anomaly from the profile shown in Fig. 18 (a). Distributions of a-

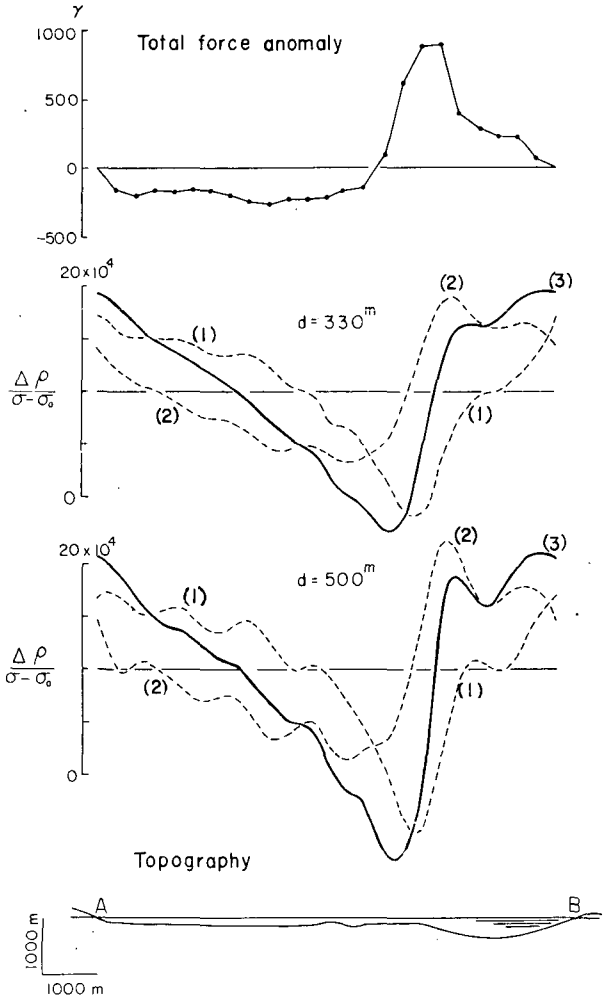

Fig. 19. Distribution of anomalous magnetic mass assumed to be concentrated on a plane. d denotes the depth of concentration plane bellow the lake surface.

nomalous mass which is responsbile for the observed total force anomaly are obtained as shown in Fig. 19 where the concentration plane is assumed to be situated at depths of 330 meter (maximum depth of the lake water) and 500 meter below the water surface. In the figure, curve (1) represents the distribution for the case $\Delta T_2=0$, in other words, corresponds (not the same) to the one of the horizontal component and cruve (2) represents the one for the case $\Delta T_1=0$, or corresponds to the one of the vertical compoment. And curve (3) represents the one for the case $\Delta T_1=\Delta T_2$ or equal contribution by both the components. The probable distribution ranges between curves (1) and (2), centering at curve (3). The concentration plane may be situated at a depth of 330~550 meter but may not far deeper. If we average the three curves, we may conclude that there is a deficiency of magnetic mass at the centre of the caldera and small excess of magnetic mass beneath the inner crater, or the deepest part of the lake. For reference, the distribution of the Bouguer gravity anomalies on and around the lake obtained by the present author[8] is shown in Fig. 20. In the gravity filed, a small excess of magnetic mass beneath the inner crater is not so clear.

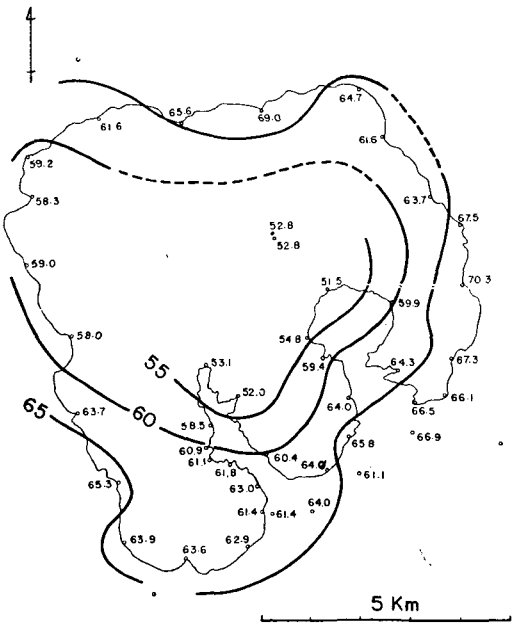

Fig. 20. Distribution of the Bouguer anomalies on and around Towada Caldera Lake. Unit is mgal.

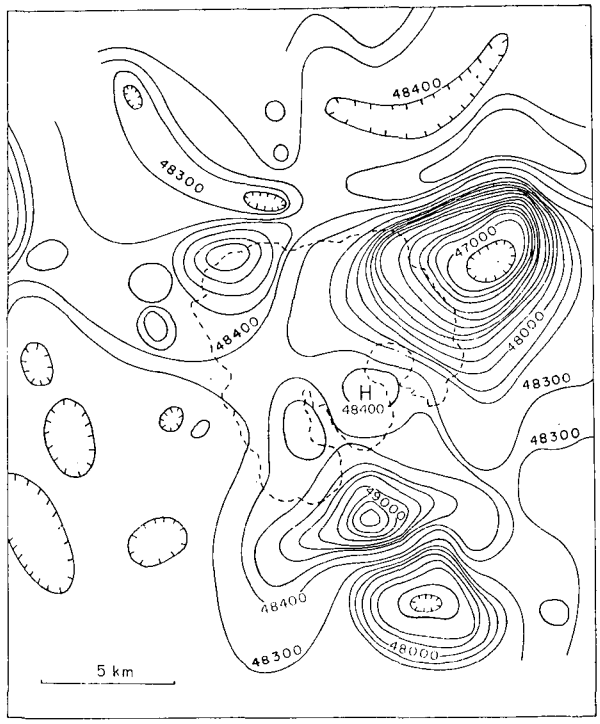

Fig. 21. Distribution of total force in gamma at a height of 1400 meter over Towada district after Y. Kato.

On the other hand, Y. Kato carried out a reconnaissance aeromagnetic survey over Towada district in 1964. One of their results is shown in Fig. 21 which is observed at a flight height of 1400 meter above sea level. A small high anomaly over the inner crater in Fig. 21 may correspond to the one observed on the water. In the figure, a large anomaly amounting to 1200 γ is very remarkable in the north-eastern coast of the lake where there is no steep volcanic cones or large gorges. The investigation of origins of this anomaly is an interesting problem in future.

Concluding remarks

As demonstrated in the exmaples, aeromagnetic surveys are liable to suffer from the topographical effects, especially in volcanic regions where there are undulations in topography. In order to get effective results in aeromagnetic surveys, a choice of flight height must be carefully made. If the

subterranean structure of a rather large depth, deeper than topographies, is aimed at by aeromagnetic surveys, it is desirable to carry out the surveys at various heights to distinguish the topographical effects and to get more information from the standpoint of potential theory. Actually Y. Kato has made his reconnaissance aeromagnetic surveys always at two different flight heights.

Acknowledgements

The author wishes to express his thanks to Professor Y. Kato, Tōhoku University, for providing the aeromagnetic maps over Towada Caldera and to Dr. H.R. Blank, the Geological Survey of U.S.A. who offered the aeromagnetic maps over Kuttyaro and Sikotu Calderas at the author's disposal. Thanks are also extended to Messrs. M. Aota and T. Maki who assisted the writer in the magnetic measurements on the lakes.

References

1) RIKITAKE, T. and HAGIWARA, Y.: Magnetic anomaly over a magnetized circular cone, Bull. Earthq. Res. Inst., **43** (1965), 509–527.
2) YOKOYAMA, I. and AOTA. M.: Geophysical studies on Sikotu Caldera, Hokkaido, Japan, Jour. Fac. Sci., Hokkaido Univ., VII, **2** (1965), 103–122.
3) STEINBERG, G.S. and RIVOSH, L.A.: Geophysical study of the Kamchatka volcanoes, Jour. Geophys. Res., **70** (1965), 3341–3369.
4) VACQUIER, V., STEENLAND, N.C., HENDERSON, R.G., and ZIETZ, I.: Interpretation of aeromagnetic maps, Geol. Soc. Amer. Mem. 47, (1951).
5) ZIETZ, I. and HENDERSON, R.G.: A preliminary report on model studies of magnetic anomalies of three-dimensional bodies, Geophysics, **21** (1956), 794–814.
6) TSUBOI, C. and FUCHIDA, T.: Relation between gravity values and corresponding subterranean mass distribution, Bull. Earthq. Res. Inst., **15** (1937), 636–649 and **16** (1938), 273–284.
7) NAGATA, T.: Magnetic anomalies and the corresponding subterranean mass distribution, Bull. Earthq. Res. Inst., **16** (1938), 550–577.
8) YOKOYAMA, I. and MAKI, T.: Preliminary report on a gravimetric survey on Towada Caldera, Tōhoku district, Japan, Jour. Fac. Sci., Hokkaido Univ., VII, **2** (1965), 251–258.